Materials Chemistry and Physics 244 (2020) 122733

Contents lists available at ScienceDirect

Materials Chemistry and Physics

journal homepage: www.elsevier.com/locate/matchemphys

Structural, elastic, electronic and optical properties of lithium halides (LiF, LiCl, LiBr, and LiI): First-principle calculations

Jingjing Wang [a], Minghua Deng [a], Yunhong Chen [a,*], Xinghong Liu [a], Wenyan Ke [a], Dandan Li [a], Wei Dai [b,**], Kaihua He [c,***]

[a] College of Computer and Information Engineering, Hubei Nomal University, Huangshi, 435002, China
[b] Department of Physics & Mechanical and Electronic Engineering, Hubei University of Education, Wuhan, 430205, China
[c] School of Mathematics and Physics, China University of Geosciences (Wuhan), Wuhan, 430074, China

HIGHLIGHTS

- The structural and elastic properties of lithium halides are investigated.
- The lithium halides are dynamical stability under ambient condition.
- The electronic band structures, density of states and electron localized function of lithium halides are analyzed.
- The absorption spectra, reflectivity spectra and dielectric function of lithium halides compounds are calculated.

GRAPHICAL ABSTRACT

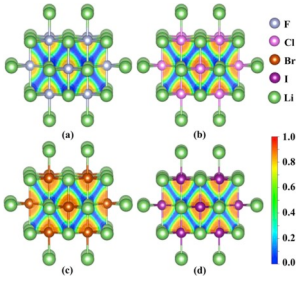

ARTICLE INFO

Keywords:
Lithium halides
First-principle calculations
Stability
Electronic properties

ABSTRACT

Lithium halides are the important members of alkali halides with important industrial application. Here, we study the structural, elastic, electronic and optical properties of lithium halides, including LiF, LiCl, LiBr, and LiI, by using the first-principles calculations. The results of elastic constants and phonon spectra show that the calculated lithium halides are all mechanical and dynamical stability under ambient condition. Using the Voigt-Reuss-Hill method, we calculate shear moduli, bulk moduli and Young's modulus of LiF, LiCl, LiBr, and LiI compounds and they are all in the order of LiF > LiCl > LiBr > LiI. The calculated structural and mechanical parameters of LiF, LiCl, LiBr, and LiI compounds correspond well with the previous reported theoretical and experimental results. The electronic properties suggest that all the calculated lithium halides have wide direct gap with strong covalent bonding. The calculated optical properties indicate that LiI is the most suitable for the reflection of ultraviolet light.

1. Introduction

Alkali metal halides are a class of alkali halides with extensive applications, including laser host materials, X-ray and neutron monochromators and radiation detector [1–6]. Lithium halides are also important members of the metal halides and have been extensively

* Corresponding author.
** Corresponding author.
*** Corresponding author.
E-mail addresses: scu_wjj@163.com (J. Wang), yunhong1619@163.com (Y. Chen), daiweiphysics@163.com (W. Dai), khhe@cug.edu.cn (K. He).

https://doi.org/10.1016/j.matchemphys.2020.122733
Received 29 September 2019; Received in revised form 19 January 2020; Accepted 26 January 2020
Available online 30 January 2020

studied in a few years' time, due to their high melting points, highly crystalline nature and strong miscibility in polar media [7–11].

Experimentally, Finch et al. have determined the lattice parameters of the potassium, sodium and lithium halides by using the electron-diffraction method, and found that crystal-size could make a noticeable effect on the lattice-dimensions [7]. Brisco and Squire have established the elastic constants of LiF by the ultrasonic methods, and then using the Houston method they estimated the Debye temperature from the values of elastic constants [8]. Lewis et al. have studied the adiabatic elastic constants of NaF, KF, LiCl, NaCl, RbCl, NaBr, RbBr, and RbI at 300 and 4.2 K by using the ultrasonic pulse-echo technique, and observed that the elastic anisotropy factor of these alkali halides increase with temperature [9]. Marshall et al. have established the elastic constants of LiBr crystal in the different temperature. Using the approximation of Betts, Bhatia and Wyman, they have also calculated the Debye temperature at 0 K and obtained a value of 276.6 K [10]. Besides the experimental studies, several theoretical calculations have also been reported. Cortona have calculated the lattice parameters, dissociation energy and bulk modulus of lithium halides by using the method for directly determining the self-consistent total energies and charge densities of solids. They have also analyzed the cause of the larger lattice constants and smaller bulk moduli, and draw a conclusion that, relative to their attractive counterpart, the approximations they chose make too high an estimate of the repulsive interactions [11]. Prencipe et al. have calculated the lattice constants, lattice energy, elastic properties and central zone phonon frequencies of LiF, NaF, KF, LiCl, NaCl, and KCl by using a periodic ab initio Hartree-Pock linear. Compared with the experimental values, the errors of these parameters increase systematically along with the size of the cation or anion increase [12]. Flórez et al. performed the study of the phase transitions and mechanical properties for alkali halides under high pressures, and draw a conclusion that the cation atomic number was the important parameter to the B1B2 transition properties [13].

Despite the many studies devoted to LiF, LiCl, LiBr, and LiI compounds, we notice that there have been no systematic studies on the stability and electronic properties of lithium halides. Thus, it now is intriguing to further study the structural stability, electronic and optical properties of LiF, LiCl, LiBr, and LiI compounds, which is essential for their practical utilization. The paper is organized as follows. In Section 2, a brief description of the theory and technical details for the calculations performed in this work is reported. The main results of the structural, elastic and electronic properties of lithium halides are presented in Section 3. Conclusions are summarized in Section 4.

2. Method

The structural optimization and electronic calculations for the lithium halides are carried out based on the density functional theory as implemented in the Vienna Ab Initio Simulation Package (VASP) [14–16]. We used the Perdew–Burke–Ernzerhof (PBE) functional for the generalized gradient approximation (GGA), and also used the local density approximation (LDA) for comparison [17–19]. The frozen-core all-electron projector augmented wave (PAW) method [20] was adopted with $1s^2 2s^1$, $2s^2 2p^5$, $3s^2 3p^5$, $4s^2 4p^5$ and $5s^2 5p^5$ treated as valence electrons for Li, F, Cl, Br and I, respectively. Accurate convergence tests are performed in order to obtain the reliable results. We choose a cutoff energy of 600 eV and fit Monkhorst-Pack k-point [21] to ensure that total energy calculations are well converged to less than 1 meV/atom. Formation enthalpies per atom ΔH of lithium halides are quantified by the reaction route as $\Delta H = [H\ (\mathrm{LiX}) - H(\mathrm{Li}) - H(\mathrm{X})]/2$. The phonon frequencies calculations are performed by using the finite displacement approach implemented in the PHONOPY program [22].

3. Results and discussion

3.1. Structural properties and thermodynamically stability

Firstly, we optimize the conventional unit cells of lithium halides, which adopt the NaCl-type structure (cubic, *Fm*-3*m*) as shown in Fig. 1. The *Fm*-3*m* phase of LiF, LiCl, LiBr, and LiI contains four LiX formula units per cell and Each X atom is coordinated by six neighboring Li atoms. Li occupy the 4a Wyckoff sites (0, 0, 0) and X atom locate at the 4b Wyckoff site (0.5, 0.5, 0.5). The calculated lattice parameter *a*, equilibrium lattice volume *V* and density ρ (both GGA and LDA values) are summarized in Table 1, along with previously reported experimental and theoretical data for comparison [7,11]. From Table 1, we find that the lattice parameter and equilibrium lattice volume correspond well with the reported data [7,11]. Moreover, the lattice parameters of lithium halides can be sorted in the order of LiF < LiCl < LiBr < LiI, which is consistent with the order of atomic radius of halogen.

3.2. Stability and elastic properties

In order to ascertain the thermodynamic stability of lithium halides, the formation enthalpies ΔH are computed and shown in Tables 1 and 2. The negative values of ΔH indicate that they are all thermodynamically stable and can be synthesized experimentally, which are confirmed by the synthesis of lithium halides [7–10]. To further establish the mechanical stability and elastic properties of lithium halides, we calculate the elastic constants (both GGA and LDA values) by a direct strain-stress method. The calculated elastic constants of lithium halides are summarized in Table 3, Table 4 and Fig. 2, which agree well with the experimental [8–10,23–25]. Interestingly, the calculations (both GGA and LDA values) show a same tendency for the three elastic constants of lithium halides with the order of $C_{11} > C_{44} > C_{12}$. For the cubic crystal, the mechanical stability criteria are given by Refs. [26–28]:

The positive values of the elastic constants, as summarized in Table 3, Table 4, Fig. 2 and Fig. S1 (see the Supporting Information), clearly suggest that the four compounds are all satisfied the mechanical stability criteria indicating mechanical stability. Furthermore, we have also checked their dynamical stabilities by calculating the phonon dispersion curves. The phonon dispersion relations are illustrated in Fig. 3. From Fig. 3, we can see that no negative phonon frequencies detected over the whole Brillouin zones, implying the dynamical stability of lithium halides. A further analysis of the projected phonon density of states (PHDOS) for lithium halides show that the Li atoms in LiF and LiI have the highest and lowest vibrational frequency of 14.75 THz and 7.36 THz respectively. For LiBr and LiI compounds, Low-frequency vibrations are mostly related to Li atoms, while higher-

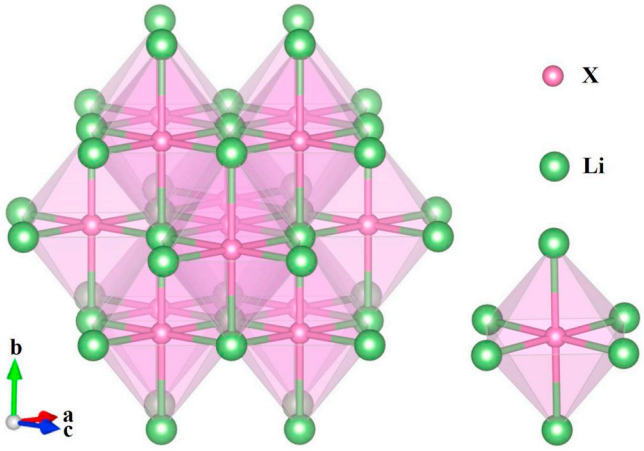

Fig. 1. Crystal structures of lithium halides.

Table 1
Calculated lattice parameter, volume, mass density and relatice enthalpy of formation for LiF and LiCl compared with experimental and other theoretical data.

	LiF				LiCl			
	Present		Theo [11].	Exp [7].	Present		Theo [11].	Exp [7].
	GGA	LDA			GGA	LDA		
a(Å)	4.098	3.983	4.05	4.027	5.158	4.939	5.08	5.136
V (Å^3)	68.799	63.187	54.90	55.04	137.264	120.840		
ρ(g/cm^3)	2.504	2.726			2.051	2.337		
ΔH (eV)	3.83	3.81			1.79	1.76		

Table 2
Calculated lattice parameter, volume, mass density and relatice enthalpy of formation for LiBr and LiI compared with experimental and other theoretical data.

	LiBr				LiI			
	Present		Theo [11].	Exp [7].	Present		Theo [11].	Exp [7].
	GGA	LDA			GGA	LDA		
a(Å)	5.518	5.490	5.44	5.495	6.024	5.988	5.93	6.019
V (Å^3)	168.052	165.496			218.580	214.707		
ρ(g/cm^3)	3.432	3.485			4.067	4.140		
ΔH (eV)	−1.54	−1.52			−1.25	−1.22		

Table 3
Calculated elastic constants (GPa), bulk modulus B (GPa), shear modulus G (GPa), Young's modulus E (GPa), Poisson's ration v and Debye temperature Θ_D (K) of LiF and LiCl.

	LiF				LiCl			
	Present		Theo [27].	Exp [8].	Present		Theo [28].	Exp [9].
	GGA	LDA			GGA	LDA		
C_{11}	108.83	124.20	120	124.6	51.84	56.91	69.0065	60.74
C_{44}	57.29	56.91	50	64.9	24.34	29.04	27.5930	26.92
C_{12}	44.58	42.67	58.3	42.4	21.24	23.36	22.4785	22.70
B	66.00	69.85	55.917	69.9	31.44	34.54	35.2	35.4
G	45.42	52.35			20.2	23.30	23.264	
B/G	1.45	1.33			1.56	1.48		
E	110.84	125.67			49.92	57.08		
v	0.22	0.20			0.24	0.22	0.2242	
Θ_D	684.8	723.3	736	580	401.5	421.5	445.24	429

Table 4
Calculated elastic constants (GPa), bulk modulus B (GPa), shear modulus G (GPa), Young's modulus E (GPa), Poisson's ration v and Debye temperature Θ_D (K) of LiBr and LiI.

$$C_{11} > 0, C_{44} > 0, C_{11} > |C_{12}|, (C_{11} + 2C_{12}) > 0. \quad (1)$$

	LiBr				LiI			
	Present		Theo [29].	Exp [10].	Present		Theo [29].	Exp.
	GGA	LDA			GGA	LDA		
C_{11}	42.38	52.56	48.6	47.21	30.54	39.57	35.2	
C_{44}	18.89	22.79	15.4	20.52	13.66	17.42	10.5	
C_{12}	17.32	19.17	15.4	15.90	12.44	14.31	10.5	
B	25.68	30.30	28.5	26.3	18.47	22.73	22.0	
G	16.02	20.12			11.58	15.32		
B/G	1.60	1.50			1.60	1.48		
E	39.79	49.42			28.74	37.52		
v	0.24	0.23			0.24	0.22		
Θ_D	258.6	288.6			185.0	211.7		

frequency modes mainly come from the vibration of Br or I atoms.

The calculated shear modulus G, bulk modulus B, Young's modulus E and Poisson's ratio v using the Voigt-Reuss-Hill method [29,30] are listed in Table 3, Table 4, Fig. 4 and Fig. S2 (see the Supporting Information). We note that the values of shear modulus G, bulk modulus B, Young's modulus E and Poisson's ratio v (both GGA and LDA values) all can be sorted in the order of LiF > LiCl > LiBr > LiI.

3.3. Debye temperature

The Debye temperature of lithium halides (LiF, LiCl, LiBr, and LiI) can be calculated by using the formulae [31]:

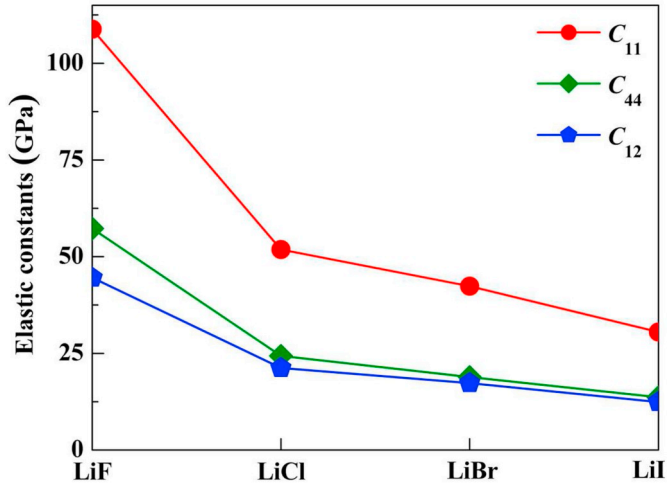

Fig. 2. The calculated elastic constants of lithium halides at GGA level.

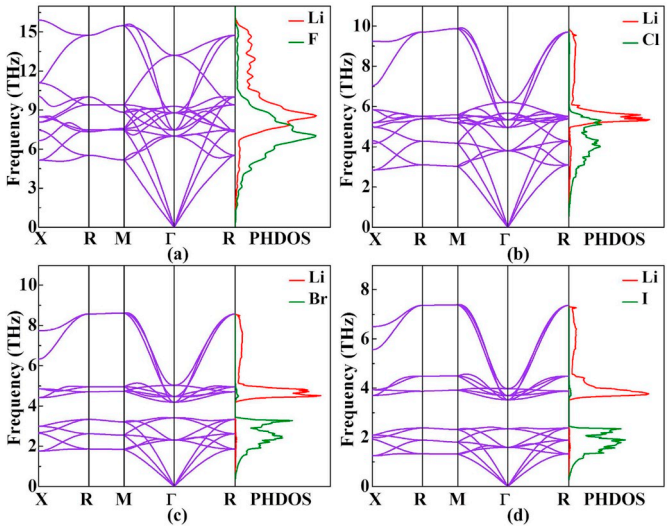

Fig. 3. The phonon dispersion curves of lithium halides at the GGA level.

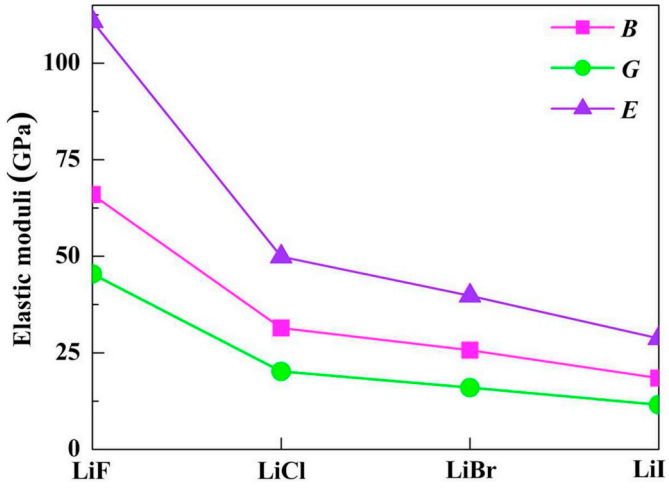

Fig. 4. The bulk moduli B, shear moduli G and Young's moduli E for lithium halides at GGA level.

$$\Theta_D = \frac{h}{k_B}\left(\frac{3nN_A}{4\pi}\right)^{1/3} V^{-1/3} v_m \tag{2}$$

where h, k_B and N_A are the Planck's constant, Boltzmann's constant and Avogadro's number, respectively. We can obtain the average sound velocity v_m using the Voigt-Reuss-Hill averaging method by the equation [30]:

$$v_m = \left[\frac{1}{3}\left(\frac{2}{v_t^3} + \frac{1}{v_l^3}\right)\right]^{-1/3} \tag{3}$$

where the v_t and v_l are the transverse and the longitudinal velocities, respectively, which can be calculated by using the Navier's equation [30]:

$$v_t = \sqrt{\frac{G}{\rho}}, v_l = \sqrt{\frac{3B + 4G}{3\rho}} \tag{4}$$

The calculated Debye temperature (both GGA and LDA values) of lithium halides are listed in Tables 3 and 4, together with the available theoretical and experimental data. We find that our calculated results correspond well with the previous reported theoretical and experimental results. The values of Debye temperature Θ_D can be sorted in the order LiF > LiCl > LiBr > LiI. Unfortunately, there are no experimental and theoretical data available related to the Debye temperature, shear modulus and Young's modulus of LiBr and LiI in the literature. Therefore, it is a first attempt in this direction and is good reference for future experiments.

3.4. Electronic properties

The electronic band structures of lithium halides are calculated (both GGA and LDA values) and shown in Fig. 5 and Fig. S3 (see the Supporting Information). The results of electronic band structures show that all the lithium halides computed are wide direct gap, due to that the bottom of the conduction band and the top of valence band are all at the gamma-symmetry point. The values of band gap of lithium halides (both GGA and LDA values), as shown in Fig. 6, can be sorted in the order LiF > LiCl > LiBr > LiI. We clearly note that the calculated results are consistent with the previous reports calculated within GGA and LDA [2,3,32,33]. In order to check the reliability of our calculations, we recalculate the band structure of lithium halides using mBJ-PBE-GGA method [34–37] (see Fig. S4 and Table S1 in the Supporting Information). The calculated results display that, for the same alkali halide, the band gap values are found to vary on the basis of three different methods (GGA, LDA and mBJ-PBE-GGA). Additionally, the band gap values of the same alkali halide can be sorted in the order LDA < GGA < mBJ-PBE-GGA. To further explain the electronic band structure of lithium halides, we have also computed the density of states (TDOSs) and partial density of states (PDOSs) (see Fig. 5). The projected density of states of lithium halides indicate that the valence band mainly formed by the p orbital of halogen atom, whereas the conduction band mainly consists of s orbital of Li and p orbital of halogen atom. It is worth noting that, for all the lithium halides, the Li 2s orbital hybridizes significantly with the p orbital of halogen atom above the fermi level, indicating the strong covalent bonding nature. The strong covalent bonding between Li and neighboring halogen atoms also can be seen from the calculated electron localized function (ELF) (see Fig. 7). The isosurface plots indicate the strong covalent bonding between Li and neighboring halogen element of lithium halides. As a consequence of these strong covalent bonding, the structural stabilities of lithium halides would be surely increased.

3.5. Optical properties

The wide band gaps materials have different applications such as optical switches, optical filters, wave guides and reflector [38–43] Due

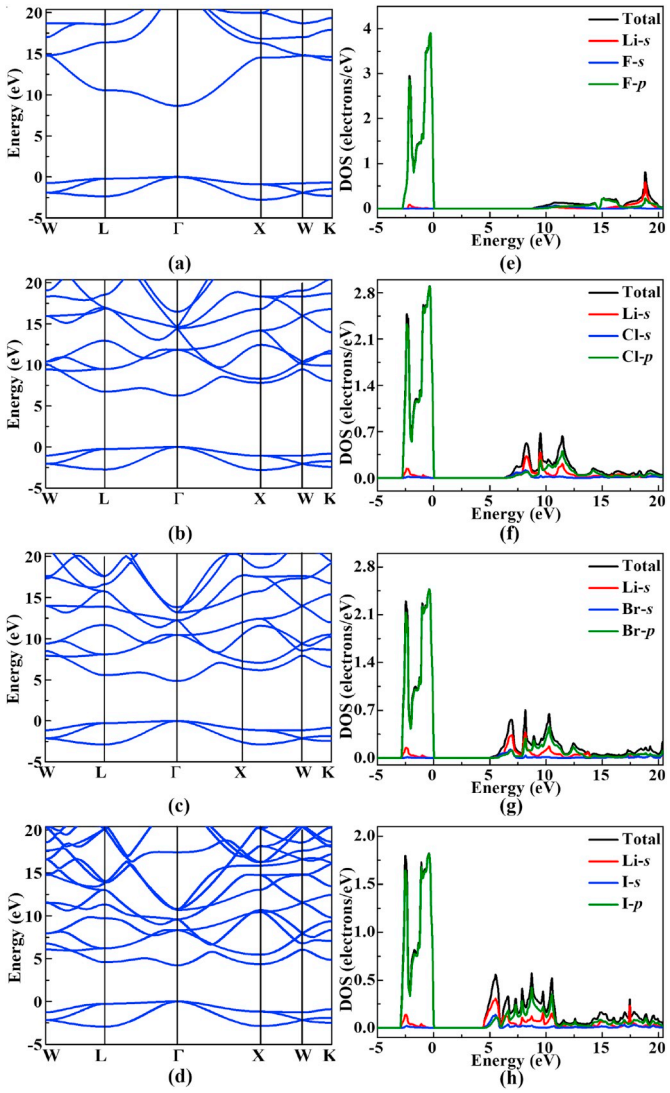

Fig. 5. The energy band structure and density of states of lithium halides at GGA level. (a) and (e) for LiF, (b) and (f) for LiCl, (c) and (g) for LiBr, (d) and (h) for LiI.

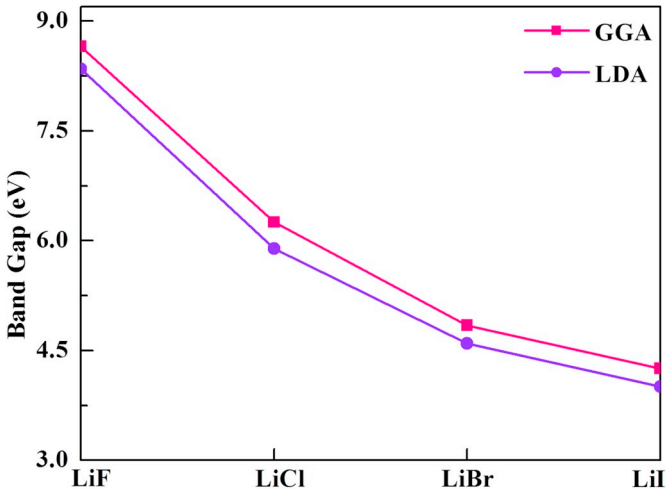

Fig. 6. The calculated band gap of lithium halides.

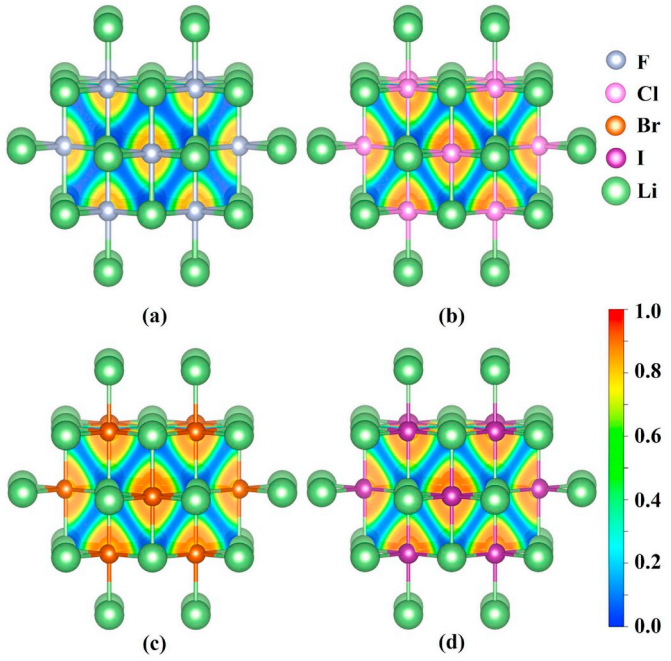

Fig. 7. The electron localized function of lithium halides. (a) LiF, (b) LiCl, (c) LiBr, (d) LiI.

to the results for electronic band gap of lithium halides are obtained, the optical properties have been calculated. The macro-optical response functions of solids in the linear response range can be estimated by using the refractive index $N(\omega) = n(\omega) + ik(\omega)$ or the dielectric function $\varepsilon(\omega) = \varepsilon_1(\omega) + i\varepsilon_2(\omega)$, where $\varepsilon_1 = n^2 - k^2$, $\varepsilon_2 = 2nk$ and n is the refractive index, k is the extinction coefficient. Consider the theoretical formulae below [44]:

$$\alpha \equiv \frac{2\omega k}{c} = \frac{4\pi k}{\lambda_0} \tag{5}$$

$$R(\omega) = \frac{[(n-1)^2 + k^2]}{[(n+1)^2 + k^2]} \tag{6}$$

$$\varepsilon(\omega) = \varepsilon_1(\omega) + i\varepsilon_2(\omega) \tag{7}$$

We can obtained the absorption spectra α, reflectivity spectra $R(\omega)$ and dielectric function $\varepsilon(\omega)$ of soilds. The calculated absorption spectra α, reflectivity spectra $R(\omega)$ and the real part of dielectric function $\varepsilon(\omega)$ for lithium halides are illustrated in Fig. 8. From Fig. 8 (a), we can see that from LiF to LiI, the absorption peaks have been moved to low-energy edge with the decrease of frequency. The reflectivity spectra and the real part of dielectric function of lithium halides shown in Fig. 8 indicated that the static reflectivity and static dielectric constant of LiX can be both sorted in the order of LiF < LiCl < LiBr < LiI. In the ultraviolet photon energy range as 3.3 eV~6.2 eV, the reflectivity of the four materials is sorted in the order of LiI > LiBr > LiCl > LiF. With the increase of the radius of the seven atoms, the reflectivity increases gradually, indicating that LiI is the most suitable for the reflection of ultraviolet light.

4. Conclusions

In summary, we perform systematically theoretical studies on the structural, elastic, electronic and optical properties of lithium halides by using the first-principles calculations based on the density functional theory. The calculated results indicate that the four halides are thermodynamically, mechanical and dynamically stable. The estimated Debye temperature can be sorted in the order of LiF > LiCl > LiBr > LiI >

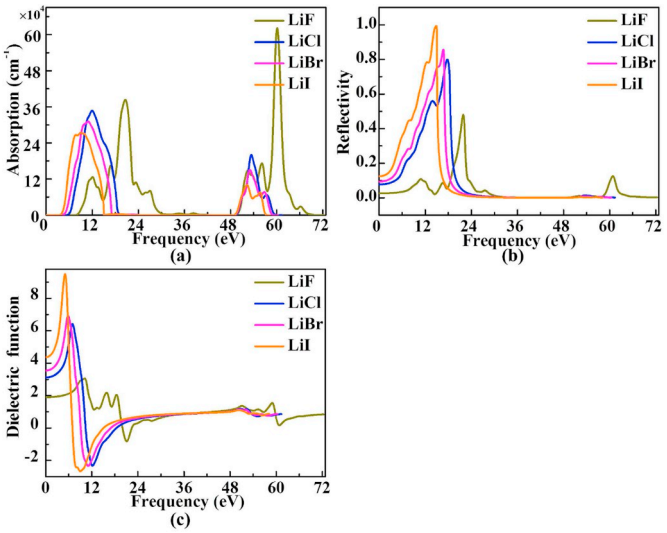

Fig. 8. The calculated absorption spectra, reflectivity spectra and real part of dielectric function of lithium halides at GGA level.

Li. The band structures, density of states and electron localized function demonstrate that all the compounds of lithium halides computed have wide direct gap with strong covalent bonding. The calculated optical properties of lithium halides indicate that LiI is the most suitable for the reflection of ultraviolet light. These results are expected to extend the comprehending the structural, electronic and optical properties of lithium halides.

Declaration of competing interest

The authors declare that they have no competing interests.

Acknowledgements

This work is supported by the National Natural Science Foundation of China (Grant Nos. 11604175, 11747139 and 11804031), the Open Research Projects of Wuhan Huada (No. NERCEL-OP2015001), the Provincial Teaching Research Project in Hubei province of China (Grant No. 2017369) and the Science and Technology Plan Projects in Qinghai province of China (Grant No: 2014-ZJ-942Q).

Appendix A. Supplementary data

Supplementary data to this article can be found online at https://doi.org/10.1016/j.matchemphys.2020.122733.

References

[1] Z. Liu, Z. Hou, F. Ruan, Y. Yin, J. Zhang, Effect of libr addition on the electrochemical performance of La_2Mg_{17}/Ni composites prepared by ball milling, J. Alloys Compd. 624 (2015) 68–73.
[2] M. Shahrokhi, B. Mortazavi, Lithium halide monolayer sheets: first-principles many-body calculations, Comput. Mater. Sci. 143 (2018) 103–111.
[3] G. Lanaro, G. Patey, Crystal structures of model lithium halides in bulk phase and in clusters, J. Chem. Phys. 146 (2017) 154501.
[4] L. Rycerz, E. Ingier-Stocka, M. Berkani, M. Gaune-Escard, Thermodynamic and transport properties of the $PrBr_3$-RbBr binary system, J. Alloys Compd. 501 (2010) 269–274.
[5] E. Ingier-Stocka, L. Rycerz, S. Gadzuric, M. Gaune-Escard, Thermal and conductometric studies of the $CeBr_3$-MBr binary systems (M = Li, Na), J. Alloys Compd. 450 (2008) 162–166.
[6] K. Haddadi, A. Bouhemadou, L. Louail, D. Maouche, Ab initio study of structural, elastic, and high-pressure properties of rubidium halides RbX (X = F, Cl, Br and I), Phase Transitions 82 (2009) 266–279.
[7] G. Finch, S. Fordham, The effect of crystal-size on lattice-dimensions, Proc. Phys. Soc. 48 (1936) 85–94.
[8] C. Briscoe, C. Squire, Elastic constants of LiF from 4.2°K to 300°K by ultrasonic methods, Phys. Rev. 106 (1957) 1175–1177.
[9] J. Lewis, A. Lehoczky, C. Briscoe, Elastic constants of the alkali halides at 4.2°K, Phys. Rev. 161 (1967) 877–887.
[10] B. Marshall, C. Cleavelin, Elastic constants of LiBr from 300° to 4.2°K, J. Phys. Chem. Solid. 30 (8) (1969) 1905–1908.
[11] P. Cortona, Direct determination of self-consistent total energies and charge densities of solids: a study of the cohesive properties of the alkali halides, Phys. Rev. B 46 (1992) 2008–2014.
[12] M. Prencipe, A. Zupan, R. Dovesi, E. Apra, V. Saunders, Ab initio study of the structural properties of LiF, NaF, KF, LiCl, NaCl, and KCl, Phys. Rev. B 51 (1995) 3391–3396.
[13] M. Flórez, J. Recio, E. Francisco, M. Blanco, A.M. Pendás, First-principles study of the rocksalt-cesium chloride relative phase stability in alkali halides, Phys. Rev. B 66 (2002) 144112.
[14] G. Kresse, J. Furthmoller, Efficient iterative schemes for ab initio total-energy calculations using a plane-wave basis set, Phys. Rev. B 54 (1996) 11169–11186.
[15] C. Lu, M. Miao, Y. Ma, Structural evolution of carbon dioxide under high pressure, J. Am. Chem. Soc. 135 (2013) 14167–14171.
[16] C. Lu, Q. Li, Y. Ma, C. Chen, Phys. Rev. Lett. 119 (2017) 115503.
[17] J.P. Perdew, J.A. Chevary, S.H. Vosko, K.A. Jackson, M.R. Pederson, D.J. Singh, C. Fiolhais, Atoms, molecules, solids, and surfaces: applications of the generalized gradient approximation for exchange and correlation, Phys. Rev. B 46 (1992) 6671–6687.
[18] B. Hammer, K.W. Jacobsen, J.K. Ngrskov, Role of nonlocal exchange correlation in activated adsorption, Phys. Rev. Lett. 70 (1993) 3971.
[19] P.E. Blöchl, Projector augmented-wave method, Phys. Rev. B 50 (1994) 17953–17979.
[20] H.J. Monkhorst, J.D. Pack, Special points for brillouin-zone integrations, Phys. Rev. B 13 (1976) 5188–5192.
[21] A. Togo, F. Oba, I. Tanaka, First-principles calculations of the ferroelastic transition between rutile-type and $CaCl_2$-type SiO_2 at high pressures, Phys. Rev. B 78 (2008) 134106.
[22] Z.H. Levine, J.H. Burnett, E.L. Shirley, Photoelastic and elastic properties of the fluorite structure materials, LiF, and Si, Phys. Rev. B 68 (2003) 155120.
[23] H. Hou, F. Kong, J. Yang, S. Wan, S. Yang, Ab initio investigation on the elastic, dynamical and thermodynamic properties of LiCl, Physica B 428 (2013) 5–9.
[24] N.A. Smirnov, Ab initio calculations of the thermodynamic properties of LiF crystal, Rhys. Rev. B 83 (2011), 014109.
[25] J. Haines, J.M. Léger, G. Bocquillon, Synthesis and design of superhard materials, Annu. Rev. Mater. Res. 31 (2001) 1–23.
[26] J. Wang, X. Kuang, Y. Jin, C. Lu, X. Huang, Theoretical investigation on the structural phase transition, elastic properties and hardness of RhSi under high pressure, J. Alloys Compd. 592 (2014) 42–47.
[27] Z. Wu, E. Zhao, H. Xiang, X. Hao, X. Liu, J. Meng, Crystal structures and elastic properties of superhard IrN_2 and IrN_3 from first principles, Rhys. Rev. B 76 (2007), 054115.
[28] J. Wang, A. Hermann, X. Kuang, Y. Jin, C. Lu, C. Zhang, M. Ju, M. Si, l. Toshiaki, Exploration of stable stoichiometries, physical properties and hardness in the Rh-Si system: a first-principles study, RSC Adv. 5 (2015) 53497–53503.
[29] R. Hill, The elastic behaviour of a crystalline aggregate, Proc. Phys. Soc. 65 (1952) 349–354.
[30] Q. Chen, B. Sundman, Calculation of debye temperature for crystalline structures–a case study on Ti, Zr, and Hf, Acta Mater. 49 (2001) 947–961.
[31] Y. Du, B. Chang, H. Wang, J. Zhang, M. Wang, First principle study of the influence of vacancy defects on optical properties of GaN, Chin. Optic Lett. 10 (2012), 051601.
[32] P.K. de Boer, R.A. de Groot, Conduction bands and invariant energy gaps in alkali bromides, Eur. Phys. J. B 4 (1998) 2528.
[33] N.P. Wang, M. Rohlfing, P. Kruger, J. Pollmann, Quasiparticle band structure and optical spectrum of LiF(001), Phys. Rev. B 67 (2003) 115111.
[34] S.A. Dar, V. Srivastava, U.K. Sakalle, Structural, elastic, mechanical, electronic, magnetic, thermoelectric and thermodynamic investigation of half metallic double perovskite oxide Sr2MnTaO6, J. Magn. Magn Mater. 484 (2019) 298–306.
[35] S.A. Dar, R. Sharma, V. Srivastavac, Investigation on the electronic structure, optical, elastic, mechanical, thermodynamic and thermoelectric properties of wide band gap semiconductor double perovskite Ba2InTaO6, RSC Adv. 9 (2019) 9522.
[36] S.A. Dara, V. Srivastava, U.K. Sakalle, V. Pareye, G. Pagaref, A combined DFT, DFT + U and mBJ investigation on electronic structure, magnetic, mechanical and thermodynamics of double perovskite Ba2ZnOsO6, Mater. Sci. Eng. B 10 (2018) 217–224.
[37] S.A. Dar, V. Srivastava, U.K. Sakalle, V. Parey, Electronic structure, magnetic, mechanical and thermo-physical behavior of double perovskite Ba2MgOsO6, Eur. Phys. J. Plus 133 (2018) 64.
[38] S.O. Oseni, K. Kaviyarasu, M. Maaza, G. Sharma, G. Pellicane, G.T. Mola, ZnO:CNT assisted charge transport in PTB7:PCBM blend organic solar cell, J. Alloys Compd. 748 (2018) 216–222.
[39] G.T. Mola, E.A.A. Arbab, B.A. Taleatu, K. aviyarasu, I. Ahmad, M. Maaza, Growth and characterization of V2O5 thin film on conductive electrode, J. Microsc. 265 (2017) 214–221.
[40] G.T. Mola, S.O. Oseni, K. Kaviyarasu, M. Maaza, Co-solvent additives influence on the performance of PTB7:PCBM based Thin film organic solar cell, Mater. Today Proc. 4 (2017) 12558–12564.
[41] X.G. Mbuyise, E.A.A. Arbab, K. Kaviyarasu, G. Pellicane, M. Maaza, G.T. Mola, Zinc oxide doped single wall carbon nanotubes in hole transport buffer layer, J. Alloys Compd. 706 (2017) 344–350.

[42] G. Tessema Mola, X.G. Mbuyise, S.O. Oseni, W.M. Dlamini, P. Tonui, E.A.A. Arbab, K. Kaviyarasu, M. Maaza, Nanocomposite for solar energy application, Nano Hybrids Compos 20 (2018) 90–107.
[43] K. Kaviyarasu, G.T. Mola, S.O. Oseni, K. Kanimozhi, C.M. Magdalane, J. Kennedy, M. Maaza, ZnO doped single wall carbon nanotube as an active medium for gas sensor and solar absorber, J. Mater. Sci. Mater. Electron. 30 (2019) 147–158.
[44] Y. Du, B. Chang, H. Wang, J. Zhang, M. Wang, First principle study of the influence of vacancy defects on optical properties of GaN, Chin. Optic Lett. 10 (2012), 051601.